



**British Journal of Environment & Climate Change**  
4(4): 389-408, 2014  
ISSN: 2231-4784



SCIECEDOMAIN *international*  
[www.sciencedomain.org](http://www.sciencedomain.org)

# Stream Flow Response to Skilled and Non-linear Bias Corrected GCM Precipitation Change in the Wami River Sub-basin, Tanzania

Frank Joseph Wambura<sup>1\*</sup>

<sup>1</sup>*Department of Housing and Infrastructure Planning, Ardhi University, Box 36176, Dar es Salaam, Tanzania.*

## **Author's contribution**

*The sole author designed, analyzed and interpreted and prepared the manuscript.*

## **Article Information**

DOI: 10.9734/BJECC/2014/13457

**Original Research Article**

**Received 18<sup>th</sup> August 2014**  
**Accepted 30<sup>th</sup> October 2014**  
**Published 17<sup>th</sup> November 2014**

## **ABSTRACT**

The reliability of stream flow projection under changing climate cannot be guaranteed if the General Circulation Model (GCM) used for the projection of future climate does not predict well its past climate. In this study stream flows in the Wami River sub-basin were simulated under changing climate by the skilled and non-linear bias corrected GCM using a physically based and semi distributed rainfall runoff model, SWAT. The SWAT model was setup using the terrain, land use, soil, precipitation and temperature data. The baseline water uses were used to naturalise stream flows and the SWAT model was calibrated and validated using the historical stream flows. In addressing future runoff projections the domestic, livestock, irrigation and industrial water demands in the sub-basin were projected to the year 2039 using the current irrigation area growth rates, Tanzania vision 2025 and development plans for the Wami River sub-basin. The GCMs were incorporated in the hydrological model so as to factor in the effects of climate change. Precipitation was selected as the changing climatic variable for projection because runoff is very sensitive to precipitation as compared to other climatic variables like temperature. A total of twenty four GCMs from CMIP3 database representing twentieth century precipitation were interpolated into forty five sub-catchments in the sub-

\*Corresponding author: Email: [wafri@yahoo.com](mailto:wafri@yahoo.com);

basin and evaluated for their skills. The HADCM3 model was selected due to its highest skill score in predicting past climate. Then the HADCM3 precipitation signal of scenario A2, was corrected by Non-linear Bias Correction (NBC) in the forty five sub-catchments in the sub-basin and used to simulate future stream flow. The results of stream flow simulated using skilled and non-linear corrected HADCM3 precipitation signal shows that stream flow is projected to increase for the near term climatology (2010 – 2039).

*Keywords: Climate change; GCM precipitation change; Non-linear bias correction; skill score; wami.*

## 1. INTRODUCTION

Tanzania's economy continues to be dominated by agricultural production, which accounts to more than 50% of gross domestic product [1,2]. Among the nine (9) river basins in Tanzania, Wami River sub-basin, which is within the Wami-Ruvu basin has been identified to offer a potential area for irrigation and infield rainwater harvesting agriculture [3]. Thus, changes in freshwater resource availability are likely to be one of the most important consequences of projected 21<sup>st</sup> century climate change critically affecting sustainable development of life and livelihoods [4,5] in the Wami River sub-basin. The impacts of hydrological changes resulting from projected changes in climate may be particularly severe for the Wami River system given its role as a vital area for providing food, water and livelihoods. Previous studies of the hydrological impacts of potential climate change in Tanzania have generally focused on climate forcings from selection of GCM (s), depending on the criteria of being whether most wet or dry [6]. Although the GCM simulated temperature can be relatively consistent between GCMs, the same is not true for precipitation. Indeed, projections of future precipitation from different GCMs often disagree, even in the direction of change [7]. Therefore, there is a need to address the important issue of GCM performance score in predicting past climate before it is entrusted to be used in stream flow projection. GCM performance test can be done by several methods which compare observed and historical predictions of GCMs; some of these methods are the mean and variance method and the skill score test. The mean and variance method do not capture the extremes in the process of comparing the observed data and the GCM historical predictions. Further, the use of statistics like means and standard deviations do not allow for a comparison of the entire data distribution [8]. There is at least one major advantage of evaluating a climate model based on probability density functions (PDFs) using the skill score test. If a climate model can simulate an entire probability density function (PDF), this demonstrates a capability to simulate values that are currently rare and that may become more common in the future [9]. Thus, skill score test accounts for spatial variation in comparing modelled and measured climate parameters. However, even for the skilled GCM, its projection cannot be used without being downscaled because GCMs have coarse resolution. Most of the GCMs have a resolution of 1.3° x 2.7° latitude and longitude scale.

There are many methods available for downscaling GCM projections to a specific region or study area of interest, for discriminating between mean changes and changes in climatic variability and for ensuring consistency between climate change scenarios. The method ranges from complex procedures such as dynamical and statistical downscaling to simple approaches like bias correction methods [10,11,12]. However, Fowler et al. [12] argued that simple methods have been used for downscaling and found to be effective in simulating hydrological systems.

Dynamic downscaling is a method of extracting local scale information by developing and using limited area models (LAMs) or regional climate models (RCMs) with the coarser resolution GCM data used as boundary conditions. The basic steps are then to use the GCMs to simulate the response of the global climate. But the demerit with this method is that, the downscaling process requires computing faculties with very high computing efficiency for the computation process [10]. Therefore, this method cannot be applied in small scale or ordinary computer laboratory.

Statistical downscaling involves developing a quantitative relationship between large scale atmospheric variables (predictors) and local surface variables (predictands). From this perspective, regional or local climate information is derived by first determining a statistical model which relates large scale climatic variables to regional and local. Then the large scale output of a GCM simulation is fed into the statistical model to estimate the corresponding local and regional climate characteristics. Many statistical downscaling techniques have been developed to translate large-scale GCM output into a finer resolution. The simplest method is to apply GCM-scale projections in the form of bias correction method [12].

The most common bias correction methods for projected precipitation are simple delta method, also called Linear Bias Correction (LBC) and Non-linear Bias Correction (NBC). By LBC, the ratio of means between the future projection of GCM and its baseline is applied to the observed data to get future precipitation [11] but NBC involves the application of ratio of means between the calibrated future projection of GCM and its calibrated baseline to the observed data to get future precipitation. The main difference between LBC and NBC is that, although both approaches involve the application of GCM precipitation signal to the observed precipitation, but NBC applies the calibrated signal. To estimate the stream flow response to skilled and non-linear bias corrected GCM precipitation change, the hydrological model is the central part of linking the projected precipitation with the stream flows.

In deterministic context the hydrological models are classified as: (i) data-driven models, (ii) conceptual models; and (iii) physically based models. In this study a physically distributed rainfall runoff model known as Soil and Water Assessment Tool (SWAT) was used. This is because of the extensiveness of the sub-basin as well as the need to incorporating most of the sub-basin features in the modelling activity. SWAT is one of the common physically distributed models. It is a continuous-time distributed simulation watershed (catchment or sub-basin or basin) model [13]. SWAT is described in detail by Neitsch et al. [14], so only a brief summary of the model is provided here. SWAT was developed to predict the effects of alternative management decisions on water, sediment and chemical yields with reasonable accuracy. It uses readily available inputs, thus minimum data are required to make a run. SWAT is computationally efficient, thus simulation of very large watersheds or a variety of management strategies can be performed without excessive investment of time or money. SWAT provides an option of estimating surface runoff using the SCS curve number procedure [15]. The SCS curve number is a function of the soil's permeability, land use and antecedent soil water conditions [15]. A minimum data requirement in estimating the potential evapotranspiration is also an advantage of using SWAT model, because it incorporates the Hargreaves method which requires only air temperature in estimating potential evapotranspiration [14]. SWAT is capable of simulating a number of climate options. Climate change can be simulated with SWAT by manipulating climatic variables (precipitation, etc.) that are read into the model in each sub-catchment. It also has a less time-consuming method in setting adjustment factors for the various climatic variables. SWAT allows the adjustment terms to vary from month to month, so that the user is able to simulate seasonal changes in climatic conditions. In Nilotic countries, including Tanzania,

Kenya, Ethiopia, Rwanda, Uganda and Burundi, SWAT model has been applied in catchments for various applications [16]. Therefore, in this study the stream flow response to skilled and non-linear bias corrected GCM precipitation change, involved setting up sub-basin SWAT model, calibration and validation of the same model. Then testing of the skilled CMIP3 climate models and bias correction of the skilled GCM followed. And finally the SWAT model was customized by the projected skilled and bias corrected GCM precipitation change to simulate the stream flow response.

## **2. MATERIALS AND METHODS**

### **2.1 The Wami River Sub-basin**

The Wami River sub-basin is located between 5°S to 7°S and 36°E to 39°E. It extends from the semi-arid areas in central Tanzania to the humid inland swamps in east-central Tanzania to the Indian ocean (Fig. 1). It encompasses an area of approximately 41,167 km<sup>2</sup>. The topography of the Wami river sub-basin ranges from 2 m to 2370 m above sea level. The upstream and downstream parts the sub-basin are separated by the Eastern Arc Mountains (Nguru, Ukaguru and Rubeho mountain ranges). The Wami River sub-basin has three major catchments: Kinyasungwe, Mkondoa and Wami. Each catchment has a downstream flow gauging station, namely 1GD-Godegode, 1G1-Dakawa, and 1G2-Mandera, respectively (Fig. 1). However, this study used only the 1G2 – Mandera gauge in calibration and validation of the hydrologic model due to the length of its readily available historical records as compared to other gauges. Two representative rainfall stations (9536017-Ikombo and 9636018 -Ukaguru forest) were also used to address the rainfall variability within the sub-basin.

The sub-basin has an average rainfall of 550 to 1000 mm per annum. There are two rainfall zones in the sub-basin, the western and south–west part falls within the unimodal rainfall zone (one wet period in December, January, February, March and April (DJFMA)) and the east and north–east part of the sub-basin falls within the bimodal rainfall zone (two wet periods, first rains in October, November and December (OND) and second rains in March, April and May (MAM)). Kinyasungwe catchment falls within the unimodal rainfall zone, whereas Mkondoa and Wami catchments fall within the bimodal rainfall zone. The mean annual temperature in the sub-basin ranges from 12 to 24 degree Celsius. The low lands are warm whereas the highlands are cold. The main uses of water in Wami River sub-basin are domestic, livestock, industrial and irrigation.

### **2.2 Data Used**

In this study, data used for setting up the hydrological model were land cover (shapefile format) of scale of 1:250,000 from the Africover Land cover Classification and Natural Resource Services, FAO (1997); soil (shapefile format) of scale of 1:2,000,000 from the soil and terrain database for southern Africa developed by International Soils Reference and Information Centre, ISRIC, (2003); Digital Elevation Model (raster) of 90m resolution downloaded from the USGS/NASA STRM-DEM (2007); verified stream network of Wami River from the Ministry of Water (MoW); daily rainfall and temperature data from the Tanzania Meteorological Agency (TMA); Population data (shape file) from National Bureau of Statistics (NBS); measured stream flows at 1G2 –Mandera and water uses (irrigation and industrial water uses) from Wami-Ruvu Basin Office (WRBO) and Basin Irrigation Department (BID).

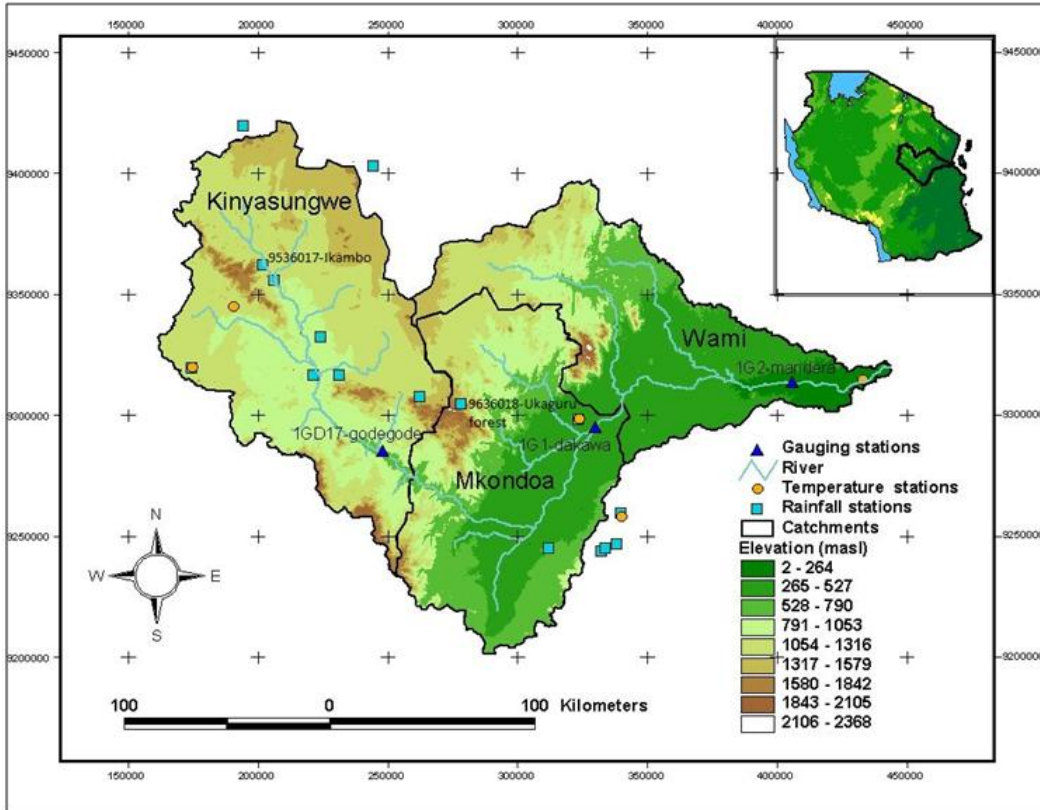


Fig. 1. Wami river sub-basin

Data used for climate customisation in the hydrological model was projected precipitation from a skilled and non-linear bias corrected GCM. For skill score test, 24 GCMs precipitation with resolution ranging from 150 to 300 km<sup>2</sup> were downloaded from the CMIP3 database in the NetCDF format.

### 2.3 Hydrologic Modelling

First, the sub-basin was divided into forty five (45) sub-catchments using the DEM which was burnt in with the verified river network dataset and the topography of each sub-catchment was derived from the same DEM, then land cover and soil were used to generate default flow parameters.

Secondly, rainfall and temperature data were used to drive the Wami River sub-basin climate. The average baseline climatological domestic, livestock, irrigation and industrial water uses were distributed in sub-catchments to naturalize stream flows. Computation of evapotranspiration was done using the Hargreaves method and the flows were routed using the Muskingum algorithm. SWAT model used water balance equation (Equation 1) as a driving force in the sub-basin [14].

$$SW_t = SW_0 + \sum_{i=1}^t (R_{day} - Q_{surf} - E_a - W_{perc} - Q_{gw}) \quad (1)$$

Where  $SW_t$  and  $SW_o$  are final and initial soil water content (mm/d) respectively;  $t$  is the time (day);  $R_{day}$  is the precipitation (mm/d);  $Q_{surf}$  is the runoff (mm/d);  $E_a$  is the evapotranspiration (mm/d);  $W_{perc}$  is the percolation (mm/d);  $Q_{gw}$  is the return flow (mm/d).

Finally, the stream flow data between 1978 and 1988 were used for calibration and between 1993 and 1996 for validation of the SWAT model. Data from the most downstream gauging station, 1G2-Mandera was used for calibration using the SWAT Calibration and Uncertainty Program (SWATCUP) because of its capability of calibrating the records with missing data. The procedure used in SWATCUP was Sequential Uncertainty Fitting (SUFI). This procedure was preferred over other methods because of its efficient optimization [17]. SUFI procedure is an inverse optimization approach that uses the Latin Hypercube Sampling (LHS) procedure along with a global search algorithm to examine the behaviour of objective functions. The procedure is sequential in nature, meaning that one more iteration can always be made before choosing the final estimates. The procedure has a Bayesian framework, indicating that the method operates within uncertainty domains (prior, posterior) associated with each parameter. It is a fitting procedure, conditioning the unknown parameter estimates on an array of observed values. Nevertheless, SUFI procedure is iterative, requiring a stopping rule which was provided by a critical value of a goal function, Nash-Sutcliffe coefficient [18].

In calibration and validation, the objective function (Equation 2) used for optimization was Nash-Sutcliffe coefficient (NSE). NSE provides a normalized estimate of the relationship between the observed and projected model values [19]. Legates and McCabe [20] argued that NSE is the most appropriate goodness-of-fit measures available because of its ability for physical interpretation owing to their meaningful comparison with zero (i.e., comparison with a long-term mean).

$$NSE = 1 - \frac{\sum_{i=1}^n (S_i - O_i)^2}{\sum_{i=1}^n (O_i - \bar{O})^2} \quad (2)$$

Where  $n$  is the number of records of the time series,  $S_i$  is the simulated variable,  $O_i$  is the observed variable and  $\bar{O}$  is the mean of the observed variable.

In model setup and simulation of the baseline conditions the 1980-2009 average water uses were used, while the 2010-2039 average water uses were used in simulation of the response of stream flows to climate change. Table 1 shows the summary of the baseline and future water uses used in this study. The future water uses were estimated under the consideration of Tanzania development goals [21], current population and irrigation area growth rates and development plans for Wami-Ruvu Basin, in which Wami River sub-basin is a part.

**Table 1. Summary of water uses in Wami river sub-basin**

		Population	Livestock	Irrigation	Industries
(1980-2009)	Users	1.5 mil	0.9 mil	6,722 ha	1*
	Demand (Lt/day)	38 mil	22.6 mil	1,320 mil	129.6 mil
(2010-2039)	Users	2.8 mil	1.3 mil	18,672 ha	2
	Demand (Lt/day)	72 mil	33.3 mil	2,964 mil	145 mil
	Increase	89%	47%	124%	12%

Note: mil stands for million and Lt/day means litres per day; \* number of industries (unit-less)

## 2.4 Interpolation of GCMs Grids

Since most GCMs have an average resolution of 1.3° x 2.7° latitude and longitude scale, therefore interpolation of the GCM grids to the point of interest was necessary before further use of GCM data for skill score testing and bias correction. However, there are many techniques available for interpolating GCM grids to the specific region of interest. In this study, the Inverse Distance Weighting (IDW) method was chosen to be used. IDW was selected because of the assumption that things that are close to one another are more alike than those that are farther apart. Thus, IDW assumes that each known point has a local influence that diminishes with distance, and the value at the unknown point is a weighted sum of the values of the known points. Detailed explanations of IDW in interpolation of climatic variables are found in, Zhu and Jia [22] and Lin and Yu [23].

Six points of GCM grids were found covering the Wami River sub-basin; of these points, each has its own distance from each of the 45 sub-catchments in the sub-basin. The interpolation of the six (6) grid points of GCMs to each sub-catchment used the weighting factor of two (2), such that the influence of one point relative to another is a function of inverse squared distance. Weighting factor was assumed as two (2) as used by Zhu and Jia [22] and Lin and Yu [23]. Therefore, the time series of precipitation of six (6) GCM grid points were interpolated into sub-catchments' precipitation GCM time series.

## 2.5 Skill Score Tests

The record length between 1973 and 2000 for both observed and GCM baseline precipitation was used for skill score testing. The missing observed precipitation (mm/month) from the historical record for the 45 sub-catchments were filled by the WXGEN algorithm developed by Nicks [24]. This is the weather generator embedded in SWAT.

In skill score test, probabilities were derived for observed and the 24 GCMs precipitation for all 45 sub-catchments. Then the GCMs' skill scores were determined for each sub-catchment using Equation 3 [8]. This test compares the similarity between two (2) PDFs; it allows a comparison across the entire PDF. The skill score is the cumulative minimum value of two distributions of each binned value, thereby measuring the common area between GCM and observed precipitation. If the PDF of observed precipitation is totally different from the PDF of GCM precipitation, the skill score equals zero with negligible overlap between the observed and GCM precipitation PDFs, but if the PDF for observed and GCM precipitation is exactly the same, the skill score becomes unity [8]. Therefore the skill score ranges between zero and unity. This test is a very simple measure that provides a robust and comparable measure of the relative similarity between GCM and observed PDFs.

$$\text{Skill score} = \sum_1^n \text{minimum} ( P_{o(k)} , P_{(k,r)} ) \quad (3)$$

Where n is the fixed number of bins, because in robust comparison PDFs should be of the same class marks.  $P_{o(k)}$  is a probability of monthly precipitation in a given bin from the observed data in sub-catchment, k, and  $P_{(k,r)}$  is the probability of monthly precipitation in a given bin from GCM, r, in the sub-catchment, k. Probability is computed as the relative frequency of a given bin value.

The skill score tests were done for precipitation of all 24 GCMs against observed precipitation in the 45 sub-catchments and the threshold score used was 75% as the

average value [8]. The performances of each GCM for all 45 sub-catchments across the sub-basin were used to evaluate the average, lower and upper dispersion bounds of skill scores for the GCMs. And GCM with the highest average score and the lowest range (uncertainty) between lower and upper scores across the sub-basin was selected as the most skilled GCM.

## 2.6 Non-linear Bias Correction of Skilled GCM

In bias correction of skilled GCM precipitation change, the new baseline (1980 – 2009) was chosen because it incorporates some of the strongest natural variability of climate, including the strongest El Nino Southern Oscillation (ENSO) warm event in 1997/1998 to a strong La Nina cold event in 1999/2000 [25]. And the scenario selected for prediction of near term (2010-2039) climatology was A2 because it expresses the criticality of a more divided world, independently operating, self-reliant nations, continuously increasing population and regionally oriented economic development [26].

In this study, the LBC, which is explained in detailed by Graham et al. [27], Sperna et al. [28], Eisner et al. [29] and Watabane et al. [30], was modified with the calibrated baseline and calibrated scenario GCM to obtain the NBC (Equation 4). NBC method corrects the coefficient of variation of the GCM precipitation signal [30,31,32,33,34,35]. This method is based upon transferring the calibrated monthly precipitation change between GCM baseline and GCM scenario to a daily observed time series. NBC uses only parameter,  $a$ , because it is only the ratio of precipitation variability signal which is required to modify the observed precipitation to simulate the future precipitation.

$$PCP_{future(i,j,k)} = OBS_{(i,j,k)} \times \left( \frac{GCM_{future(j,k,r)}}{GCM_{baseline(j,k,r)}} \right)^a \quad (4)$$

Where  $GCM_{baseline(j,k,r)}$  and  $GCM_{future(j,k,r)}$  are baseline and future precipitation of GCM,  $r$ , in month,  $j$ , in the sub-catchment,  $k$ , respectively.  $PCP_{future(i,j,k)}$  and  $OBS_{(i,j,k)}$  are the projected and observed precipitation on day,  $i$ , in month  $j$  in sub-catchment,  $k$ , respectively. Whereas  $a$  is the unit-less calibration parameter.

Therefore, bias correction of skilled GCM precipitation change of scenario A2 for the near term (2010-2039) climatology involved obtaining the calibration parameter,  $a$  in trying to match the monthly coefficient of variation of precipitation of the skilled GCM in the baseline period against observed precipitation [32,33,34,35] using equation 5. Then the same parameter,  $a$ , was used in equation 4 in calibration of the precipitation signal.

$$C_v(OBS_{(j,k)}) \cong C_v((GCM_{baseline(j,k,r)})^a) \quad (5)$$

Where  $C_v$  is the coefficient of variation (unit-less),  $OBS_{(j,k)}$  is the observed precipitation in month,  $j$ , in sub-catchment,  $k$ .

## 2.7 Climate Customisation in SWAT

In SWAT, climate customisation was done by adjusting factors for the precipitation variable for each of the 45 sub-catchments from January to December. The adjustment factor (Equation 6) for precipitation customisation was derived from equation 4 (NBC) so that it can

fit in equation 7, which is incorporated in the SWAT model [14]. Mathematically the substitution of equation 6 in equation 7 gives equation 4.

$$\text{adj}_{(j,k,r)} = \left( \left( \frac{\text{GCM}_{\text{future}}(j,k,r)}{\text{GCM}_{\text{baseline}}(j,k,r)} \right)^a - 1 \right) \times 100 \quad (6)$$

$$\text{PCP}_{\text{future}}(i,j,k) = \text{OBS}_{(i,j,k)} \cdot \left( 1 + \frac{\text{adj}_{(j,k,r)}}{100} \right) \quad (7)$$

Where  $\text{PCP}_{\text{future}}(i,j,k)$  and  $\text{OBS}_{(i,j,k)}$  are the projected and observed precipitation on day,  $i$ , in month,  $j$ , in sub-catchment,  $k$ , respectively. The adjustment factor,  $\text{adj}_{(j,k,r)}$  is the projected change in precipitation (%) in a given month,  $j$ , in sub-catchment,  $k$ , for GCM,  $r$ .  $\text{GCM}_{\text{baseline}}(j,k,r)$  and  $\text{GCM}_{\text{future}}(j,k,r)$  are monthly baseline and future precipitation of GCM,  $r$ , in month,  $j$ , in sub-catchment,  $k$ , respectively. And,  $a$ , is the unit-less calibration parameter.

### 3. RESULTS AND DISCUSSION

#### 3.1 Calibration and Validation of the SWAT Model

The SWAT model was calibrated and validated with daily observed historical records at the most downstream gauging station (1G2 – Mandera). The period from 1978 to 1988 was considered for calibration while the model was validated with historical records from 1993 to 1996. The NSE for calibration and validation were 70% and 74%, respectively. NSEs for both calibration and validation were considered satisfactory because Santhi et al. [36] and Benaman et al. [37] suggested that the prediction efficiency of the calibrated model can be judged as satisfactory if NSE values are greater or equal to 60%. However, Moriasi et al. [38] argued that NSE greater or equal to 65% in calibration and validation, the model performance is considered good. But Saleh et al. [39] and Rossi et al. [40], argued that NSE greater or equal to 65% the model performance is very good. However, there is no consensus on what is the appropriate criterion to be used in evaluation of model performance; therefore visual inspection of time series was used in drawing conclusion on the extent and ability of the model to mimic the reality [20].

Fig. 2 shows the time series comparison of simulated and observed daily flow in the Wami river sub-basin during the calibration period. The model captures well the low flows and some peaks, although the highest flow peak of 1411 m<sup>3</sup>/s (cms) was not well captured by the model. Looking on the other peaks before and after the highest peak, it was agreed that the highest peak might be an outlier or error resulting from flow measurements. Therefore the visual inspection of time series together with the statistical evaluation (NSE= 70%) in the calibration period was considered satisfactory. During the validation period (Fig. 3) the time series of comparison between the simulated and the observed measured stream flow at the 1G2 – Mandera gauge shows that the model captures all the peaks although there is slight over prediction of low flows in some days. The times series of comparison shows that the model is able to mimic stream flow because the simulated flow matches with the measured flow. The times series observations, together with the statistical evaluation (NSE= 74%) of the model concludes that the model is also satisfactory in the validation period.

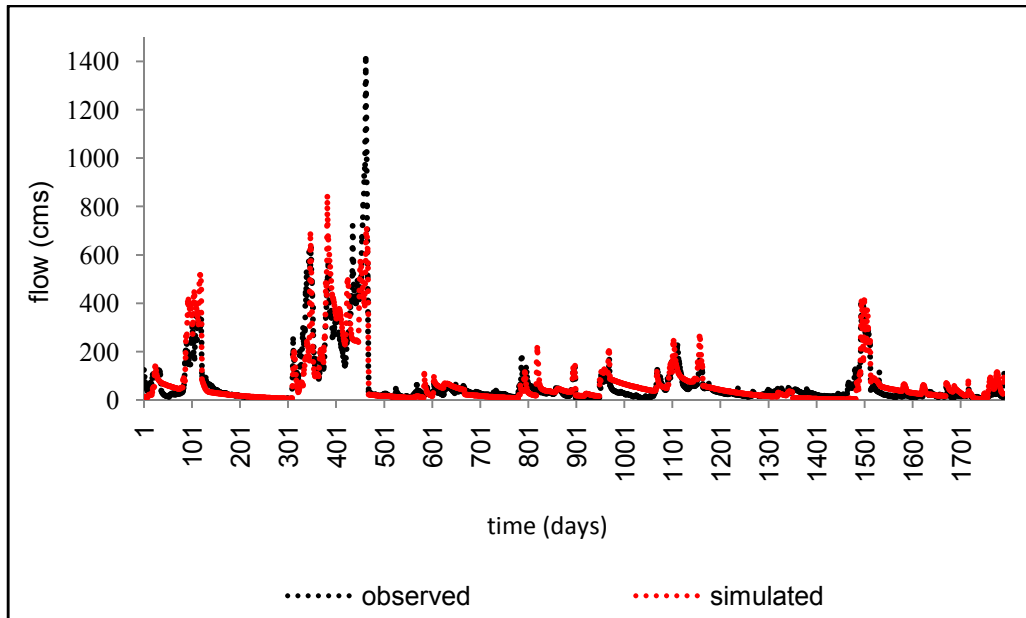


**Fig. 2. Calibration curves at 1G2-Mandera, 1978 - 1988 (missing data skipped)**

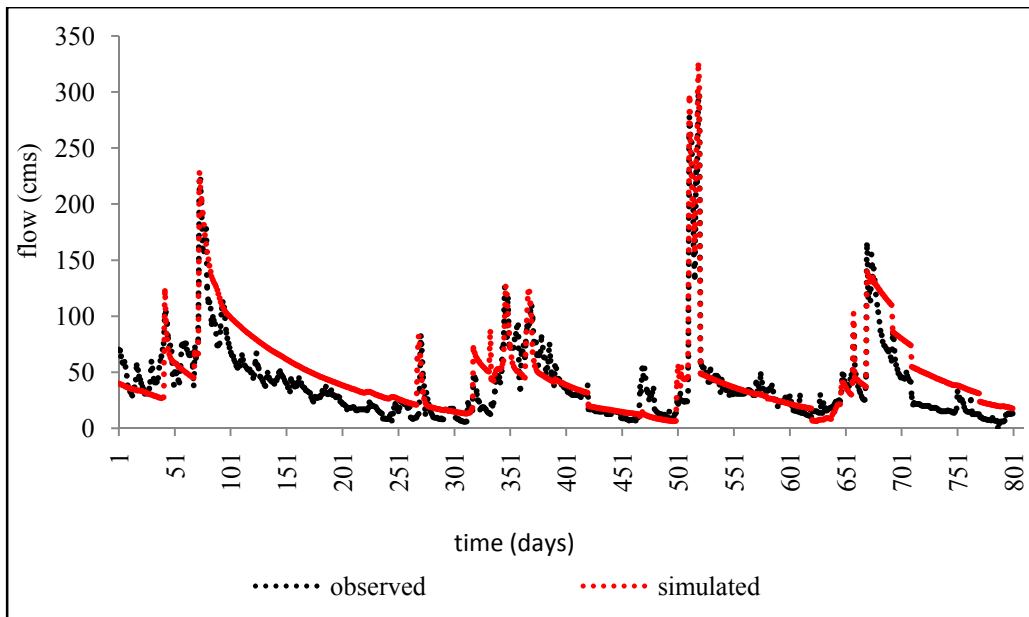


**Fig. 3. Validation curves at 1G2-Mandera, 1993-1996 (missing data skipped)**

### 3.2 Skill Score Test Results

In the skill score test, baseline/control predictions of 24 GCMs were tested against observed precipitation in each sub-catchment. And the average, lower and upper dispersion bound scores for each GCM were obtained from the sub-catchments' performances in order to represent the sub-basin skill score statistics. On average performance of GCMs across the sub-basin, it was found that GISS-EH has the lowest average sub-basin skill score, whereas

ECHAM4, ECHO, HADCM3 and HADGEM1 have average sub-basin skill scores above the threshold of 75.0% (Fig. 4). Among the four GCMs with skill scores above the threshold value, HADCM3 has the highest average sub-basin skill score of 79.0%. The other GCMs namely, ECHAM4 and ECHO both have the same average sub-basin skill score of 75.5%, but HADGEM1 has the average sub-basin skill score of 76.0%. Depending on the highest performance of GCMs across the sub-basin, it is obviously that HADCM3 was supposed to represent the future climate of the sub-basin. But nevertheless, the uncertainty of GCM performance across the sub-basin was also considered.

Uncertainty range was considered to be the interval between the upper and lower dispersion bounds of the skill scores of the 45 sub-catchments in the sub-basin. Statistically, it is twice the standard deviation of the skill scores. The uncertainty range measures the amount of variation or dispersion of the sub-catchments' skill scores from the average sub-basin skill score. A low range indicates that many sub-catchments' skill scores tend to be very close to the average sub-basin skill score; a high uncertainty range indicates that many sub-catchments' skill scores are spread out over a large range of scores. Therefore GCM with the lowest uncertainty range is the one which predicts well the natural variability of precipitation in the sub-basin, because it has the ability to model the spatial distribution of precipitation. The higher value of uncertainty ranges signifies that the GCM models only some parts of the sub-basin's precipitation patterns, whereas most parts are not well modelled. The uncertainty ranges also do identify how far the average skill scores are skewed to the few high skill scores in the sub-basin. In this study the uncertainty range of 10% was considered as the maximum threshold for selection of GCMs. This means that the sub-catchments' skill scores of prediction for a particular GCM are allowed to differ by  $\pm 5\%$  from the average sub-basin skill score.

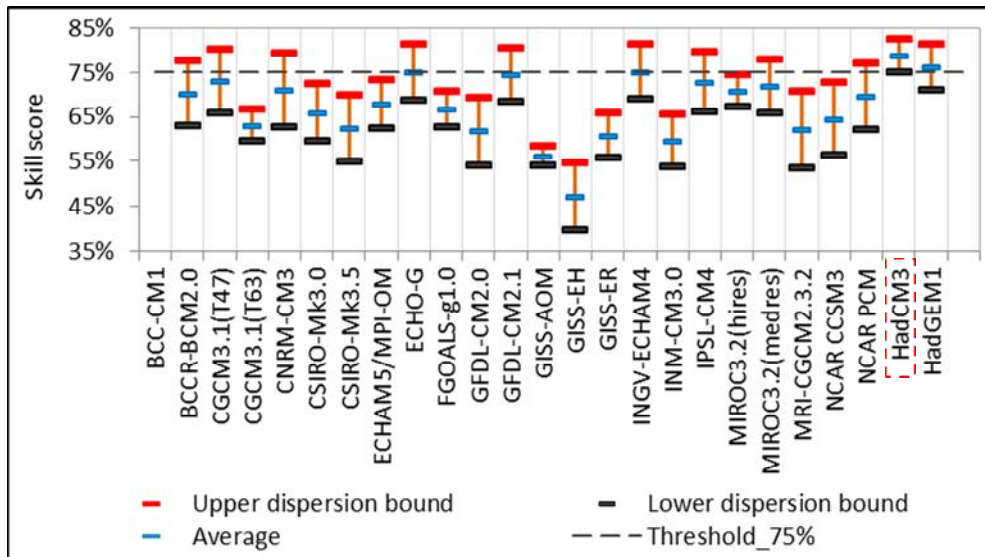


Fig. 4. Skill scores for GCMs against Observed data

Fig. 4 shows that five GCMs have an uncertainty range below 10%, these GCMs are GISS-AOM, CGCM3.1 (T63), HADCM3, MIROC3.2 (hires) and FGOALS-g1.0. GISS-AOM has the lowest uncertainty range of 4.3%, followed by CGCM3.1 (T63) and then HADCM3 with an uncertainty range of 7.3%. However the other highly skilled GCMs like ECHAM4, ECHO-G and HADGEM1 have uncertainty ranges of 12.2%, 12.8% and 10.2% respectively.

According to the uncertainty range of performance across the sub-basin, GISS-AOM, CGCM3.1 (T63), MIROC3.2 (hires) and FGOALS-g1.0 could be considered, but since their average sub-basin skill scores are far less than the threshold value, thus they were removed from consideration. Between the set of four (4) highly skilled GCMs and the set of four (4) low uncertainty range GCMs, it is only HADCM3 which is found in both sets. Therefore, HADCM3 was selected to simulate future precipitation in the Wami river sub-basin. However, the skill score test, like any other performance or efficiency measures of a model, has to be supported by visual inspection of PDFs of GCM and measured precipitation. Fig. 5 shows that, the PDFs of HADCM3 and measured precipitation matches very well from the average to high precipitation, although there is slight under prediction of low precipitation (<28 mm/month). This means HADCM3 slightly under predict “drizzle” in the Wami River sub-basin.

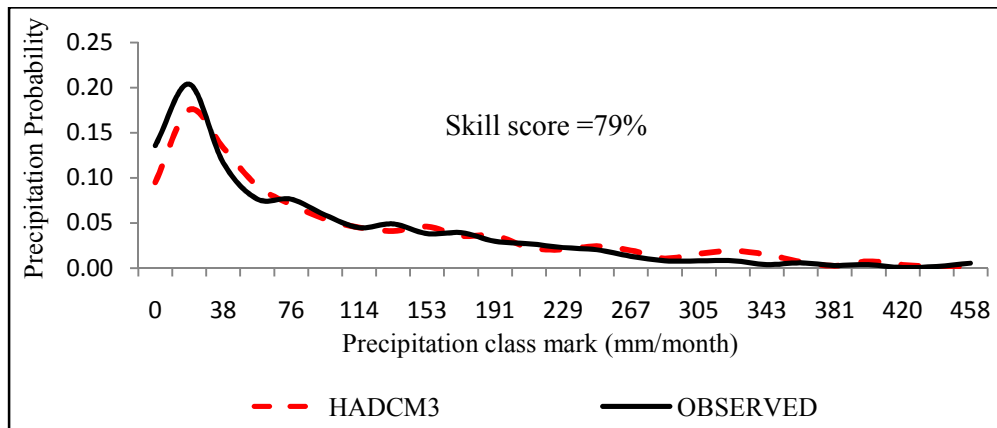


Fig. 5. GCM against Observed data

### 3.3 Measured and HADCM3 Scenario Precipitation

The average measured precipitation (1980–2009) in the upstream (Kinyasungwe catchment) of sub-basin is heavy from December to April, but decreases from May to October and then start to rise again from November towards December (Fig. 6a). This part of the sub-basin falls in the unimodal rainfall zone, the representative rainfall station (Fig. 6a) in the unimodal rainfall zone shows that the heaviest rainfall is experienced in DJFMA with the average measured rainfall (1980-2009) of 105 mm/month at 9536017-Ikombo station. Small amounts of rainfall are experienced from June to October with 11 mm/month in average. The temporal variability of measured rainfall (1980-2009) is in the range of  $\pm 62$  mm/month. The HADCM3 scenario (2010-2039) at 9536017-Ikombo station (Fig. 6b) shows that the heaviest precipitation is projected to be in March with a magnitude of about 300mm/month. Fig. 6b shows that an average increase in precipitation is projected (2010-2039) for the DJFMA period; and it is estimated to be around 106%, whereas an average decrease from June to November is projected in the magnitude of 25%.

Fig. 6c shows that, the measured precipitation in the downstream part of the sub-basin (Mkondoa and Wami catchments) is heavy in the periods of MAM and OND. This is because this area experiences bimodal rainfall. The measured precipitation at 9636018 - Ukaguru forest station (representative rainfall station in the bimodal area of the sub-basin) has an average (1980-2009) amount of 74 mm/month in the MAM season and 73 mm/month in the OND season. The average rainfall in the little rain period of June to September is 39

mm/month and the heaviest rainfalls are found between March and April in the case of MAM season whereas in the OND period, heavy rainfalls are in December. The average temporal variability of measured precipitation (1980-2009) ranges between  $\pm 78$  mm/month. The scenario predictions at 9636018 - Ukaguru forest station (Fig. 6d) shows that the heaviest precipitation (2010-2039) is projected to be in April with the magnitude of about 191 mm/month for the MAM season and in November (97 mm/month) for the case of OND season. In the MAM season the average increase in precipitation is projected to be 100% and from June to September the decrease in precipitation is projected to be 45%, but OND average precipitation is projected to decrease by 9%.

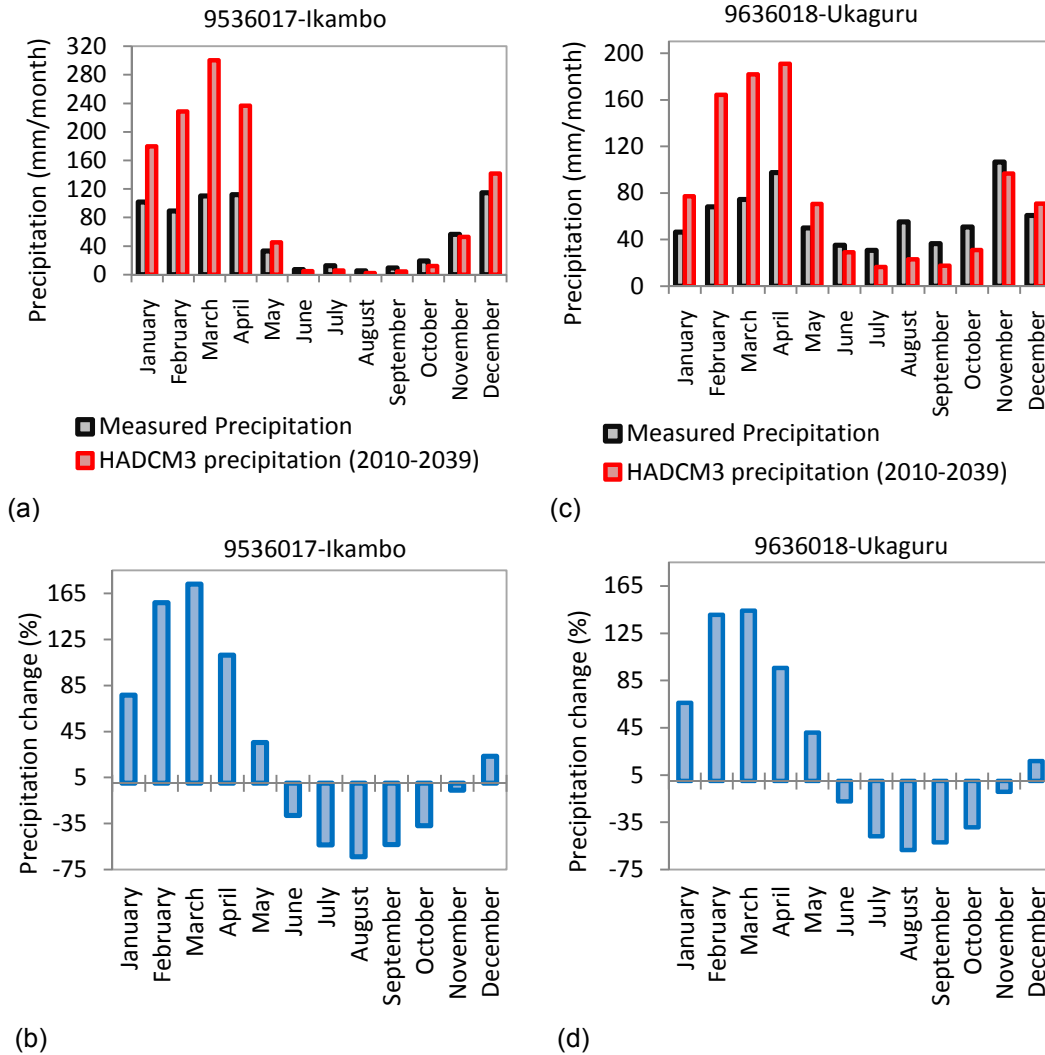


**Fig. 6. Average precipitation of representative stations**

In comparing precipitation of the upstream and downstream parts of the sub-basin, it is found that the Kinyasungwe catchment has one season of rainfall and the average annual measured rainfall (1980-2009) is around 670 mm but the Mkondoa and Wami catchments, which have two seasons of rainfall, have average annual rainfall amounts of 713 mm. The HADCM3 average annual increase of precipitation (2010-2039) is projected to be 81% in the

upstream and 36% in the downstream. The temporal variability of measured rainfall in the Mkondoa and Wami catchments is larger than that of Kinyasungwe catchment; this is partly contributed by the presence of two seasons of rainfall in the downstream part. However, the topography shows that the upstream part of the sub-basin is on the leeward, whereas the downstream part is on the windward side of the Eastern Arc Mountains. Therefore, the influence of Indian Ocean cyclonic rains is thought to be blocked by the Eastern Arc Mountains in reaching the upstream part of the sub-basin. Hence, for this reason, more rain days are encountered on the downstream part compared to the upstream part. HADCM3 prediction (2010-2039) shows that, pattern of temporal variability is the same as the one of the measured rainfall and both upstream and downstream parts of the sub-basin exhibit decrease in rainfall between June and November but increase from December to May.

### **3.4 Stream Flow Responses**

Upstream of the sub-basin (Fig. 7a) shows that, the patterns for average baseline flow (1980-2009) and the average HADCM3 projected flow (2010-2039) are similar. Both flow curves show that, stream flow at 1GD17- Godegode is high from December to May and recedes towards September. However, there is a slight increase of stream flow in October towards November. The maximum average baseline flow occurs in April ( $70 \text{ m}^3/\text{s}$ ) whereas the minimum average baseline flow occurs in August ( $0.6 \text{ m}^3/\text{s}$ ). For HADCM3 flow projection, the average maximum projected flow occurs in April and the minimum average projected flow occurs in October. Fig. 7a also shows that, HADCM3 projects a high increase ( $+392 \text{ m}^3/\text{s}$ ) in flow from February to August as the result of MAM rainfalls, but a decrease ( $-39\%$ ) in flow is projected from October to December. However, there is a slight increase of flow in January. The sudden deep drop of flow is projected in October, this is the most severe decrease ( $-99\%$ ) of flow projected by the HADCM3 in the upstream of Wami River sub-basin.

Fig. 7b shows that, at 1GD17 the baseline flow experience a slight lag between peak of precipitation and peak of flow due to the time of concentration for runoff to reach the outlet of the Kinyasungwe catchment. However, the bank storage recharge, groundwater recharge and infiltrations in the catchment are also thought to contribute to this lag in flow. This lag in flow is not experienced in the case of projected flow because HADCM3 projects a high increase in precipitation, thus the bank storage, groundwater storage and infiltrations saturate earlier than in the case of baseline flow (Fig. 7b).

At 1G1-Dakawa, in the Mkondoa catchment, the average baseline flow has the same pattern as the HADCM3 average projected flow (Fig. 8a). The highest average baseline flow occurs in March ( $56 \text{ m}^3/\text{s}$ ) and the lowest occurs in October ( $8 \text{ m}^3/\text{s}$ ). The highest average HADCM3 projected flow (2010-2039) occurs in April and the lowest occurs in November. HADCM3 projects a very high increase in stream flow from January to December in Mkondoa catchment as the results of heavy projected precipitation in the OND and MAM periods. The highest average increase in flow is projected ( $+581 \text{ m}^3/\text{s}$ ) in April and the lowest increase is projected in December ( $+75 \text{ m}^3/\text{s}$ ).

From Fig. 8b, both baseline and projected precipitation peaks in April, but the baseline flow peaks in March. Thus the lag between peak of precipitation and peak of flow is only on the baseline condition, because the HADCM3 projects a flow peak in April when the precipitation peaks. The lag in peak of baseline flow is thought to be caused by losses of water out of the streams and in the catchment as bank storage, infiltrations in the catchment as well as the groundwater recharge. However, the lag in peak of baseline flow in April also occurs in the Kinyasungwe catchment, therefore this signal of the delay is transferred to the Mkondoa

catchment from further upstream (Kinyasungwe catchment). The same effect on the peak flow also causes the low flow to lag by the same duration (Fig. 8b).

Despite the Mkondoa catchment having the OND season, but the effects of these rains, lag to the end of the season for both baseline and projected flows. Fig. 8b shows that the lag is even extensive for the projected flows because in the OND period, the HADCM3 predicts decrease in precipitation from June to November (Fig. 8b). However, water losses as bank storage recharge, groundwater recharge, irrigation abstractions and infiltrations in the catchment as well as the time of concentration of runoff to reach the outlet of Mkondoa catchment are also thought to contribute to the lag in peak of flow resulting from the OND rainfall.

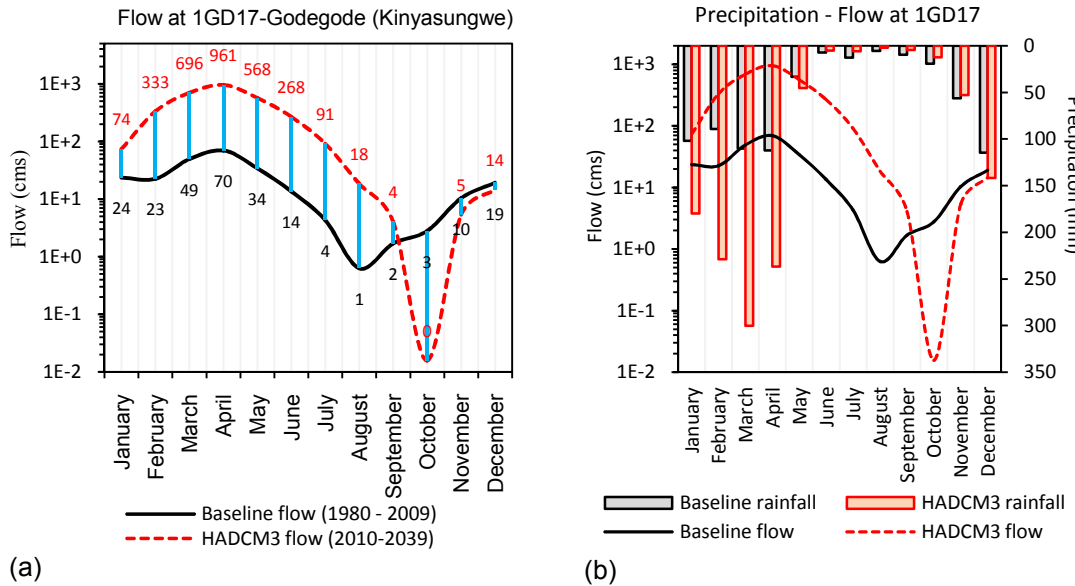


Fig. 7. Flow response at 1GD 17

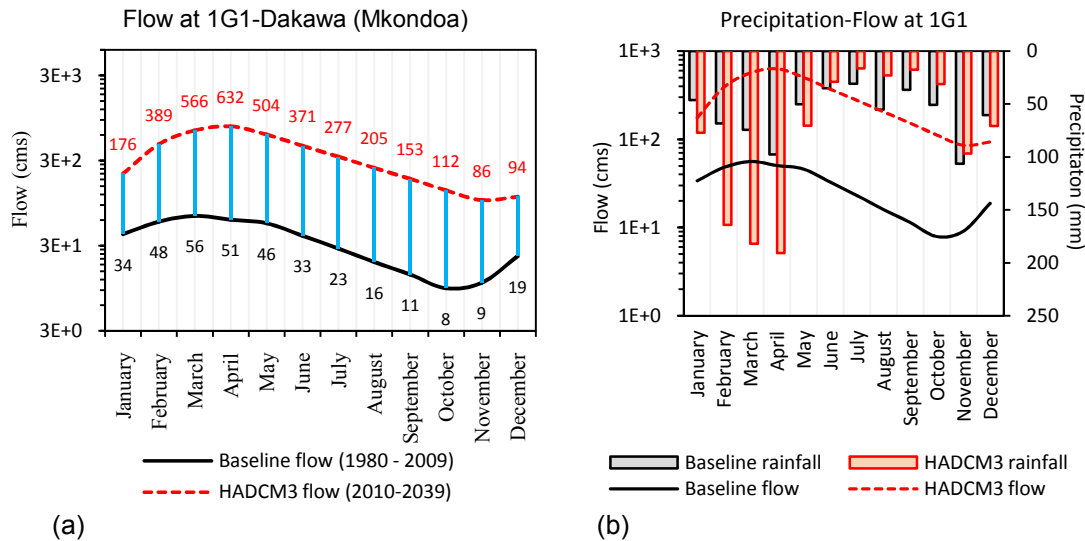
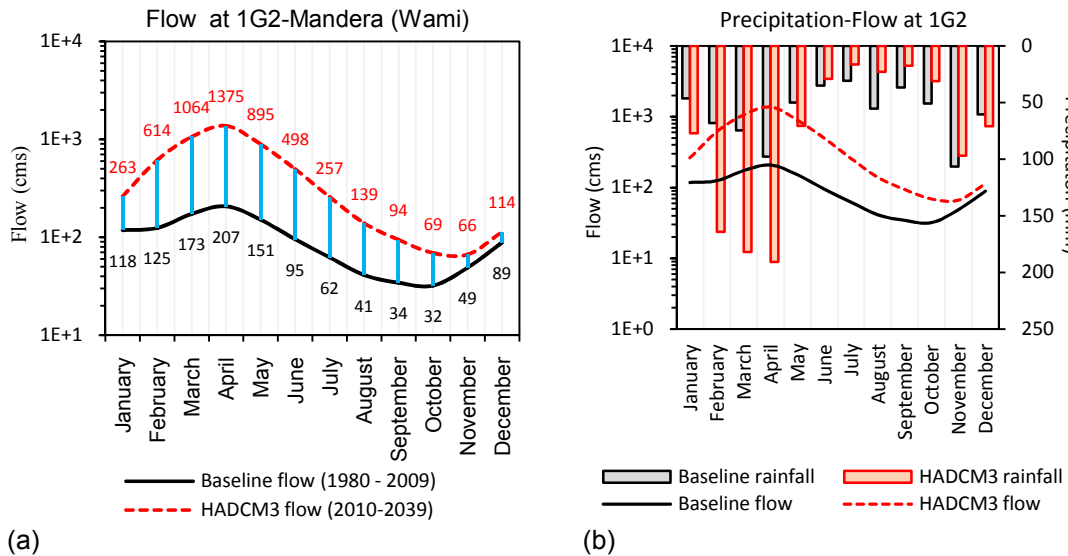


Fig. 8. Flow response at 1G1

1G2-Mandera is the most downstream flow gauge station, which collects all the stream flows from the Wami River sub-basin before they flow into the Indian Ocean. The minimum baseline flows occur in October with the magnitude of  $32\text{m}^3/\text{s}$ , whereas the maximum baseline flows occurs in April with the magnitude of  $207\text{m}^3/\text{s}$  (Fig. 9a). However, Fig. 9a also shows that, HADCM3 predicts high increase in flow throughout the year from the sub-basin; this flow results from the heavy rainfall in the MAM period. The highest increase is projected to occur in April ( $+1168\text{m}^3/\text{s}$ ) and the lowest increase is projected in November ( $+17\text{m}^3/\text{s}$ ).

Fig. 9b shows that, during the MAM period, there is not lag between peak of precipitation and peak of flow for both baseline simulations and HADCM3 projections. However, like the Mkondoa catchment, the Wami catchment also experiences the lag in the peak of flows resulting from the OND rains for both baseline and projected flows (Fig. 9b). The lag in flow in the Wami catchment is also extensive in the case of the projected flow because in the OND period, the HADCM3 predicts a decrease in precipitation. However, similar water losses from streams as in the Mkondoa catchment are also thought to be happening in the Wami catchment.



**Fig. 9. Flow response at 1G2**

The average annual baseline and projected stream flows from the Kinyasungwe catchment are  $21\text{m}^3/\text{s}$  and  $253\text{m}^3/\text{s}$  respectively (Fig. 10). Fig. 10 also shows that, the average annual stream flow from the Mkondoa catchment for baseline and projected flows are  $29\text{m}^3/\text{s}$  and  $297\text{m}^3/\text{s}$  respectively. From the Wami catchment, the average annual stream flow is the net flow from the whole sub-basin. The average annual flows from the sub-basin for baseline and projected cases are  $98\text{m}^3/\text{s}$  and  $454\text{m}^3/\text{s}$  respectively (Fig. 10). The average annual flow in the Wami River sub-basin is projected (2010-2039) to increase by 10 times in the Kinyasungwe and Mkondoa but the net outflow is projected to increase by 4 times. The baseline average annual flow shows that 72% of average annual flow from the Mkondoa catchment comes from the Kinyasungwe catchment outflow, whereas 30% of average annual flow from the Wami River sub-basin comes from the Mkondoa catchment outflow. In the case of projected flows, the average annual flow from the Kinyasungwe catchment outflow is 85% of the Mkondoa average annual flow, whereas from the whole sub-basin,

65% of average annual flow comes from the Mkondoa catchment. These quantities shows that at the baseline conditions 70% of the average annual outflow from the sub-basin results from the Wami catchment, whereas the projected average annual flow originating from the Wami catchment is 35% of the projected sub-basin outflow. This is the result of higher projected precipitation in the upstream part as compared to the downstream part of the sub-basin. Generally, a non-linear bias corrected HADCM3 (scenario A2) climate model projects (2010-2039) very high increase in flows in the Wami River sub-basin.

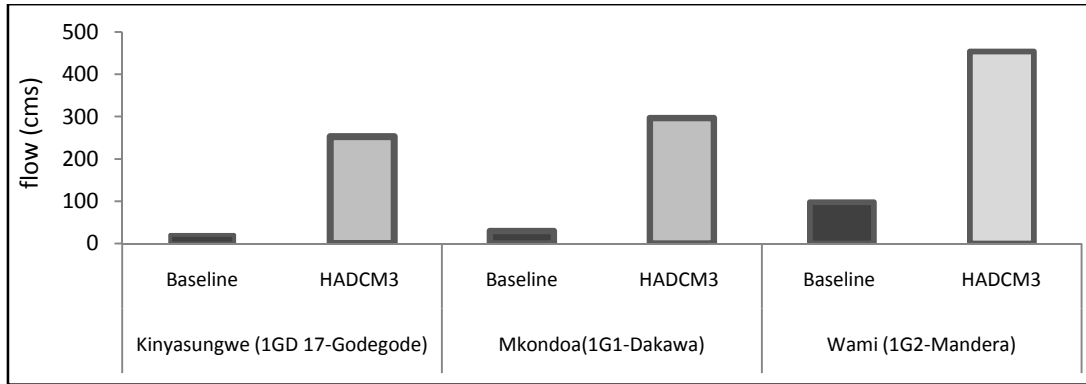


**Fig. 10. Average annual stream flow in Wami river sub-basin**

#### 4. CONCLUSION

The evaluation of climate models against observed data and the use of non-linear bias correction method are important steps in building confidence in their use for evaluation of responses from hydrological systems. This study of the response of freshwater resources within the Wami River sub-basin as a result of skill score testing and non-linear bias corrected climate model has revealed a number of important findings.

Firstly, and most importantly, it has been shown that projections of stream flow in the sub-basin are highly dependent upon the direction of projected changes in precipitation because patterns drawn by the precipitation changes are the same as those of stream flows. It is likely that such changes (particularly in high and low flows) will have important implications for both the ecological and anthropogenic development of the Wami River sub-basin.

Secondly, this study provides a useful context to previous analyses of climate change impacts on stream flow, based on a single GCM or ensemble means. Skill score test in the selection of GCM gives the credibility and reliability of the use of particular climate model in future prediction, because of its strengths in predicting the control or past period. Strong performance in a skill score test provides more confidence in a climate model in question, however, a model that does well in a skill score test could still hide major limitations in (say) the frequency of no-rain days or events that are too rare to significantly contribute to the skill score.

Non-linear bias correction is one of the very strong and simple methods for bias correction of GCM precipitation. It should be noted that there is no negligible difference between bias correction and the use of the non-bias corrected GCMs. Therefore, proper bias correction is

necessary to remove model bias in CMIP3 projections; otherwise it will generate considerable bias in the projected stream flows.

## **ACKNOWLEDGEMENTS**

This study was supported by the Enhancing Climate change adaptation in Agriculture and Water (ECAW) project. The author is gratefully thanking Prof. Siza Tumbo, Dr. Preksedis Ndomba, Dr. Victor Kongo and Mr. Charles Richard; all from the ECAW project, for supporting this study.

## **COMPETING INTERESTS**

Author has declared that no competing interests exist.

## **REFERENCES**

1. United Republic of Tanzania. Poverty and Human Development Index. Dar es Salaam: Mkuki na Nyota Publishers; 2007.
2. Nyunza G, Mwakaje EG. Analysis of round potato marketing in Tanzania: The Case of Rungwe District, Tanzania. *International Journal of Business and Social Science*. 2012;3(23):86-96.
3. Wami-Ruvu Basin Water Office. Wami Basin: A situational Analysis. Morogoro, Tanzania: Wami-Ruvu Basin Water Office; 2010.
4. Bates BC, Kundzewicz ZW, Wu S, Palutikof JP, editors. Climate change and water: Technical paper of the intergovernmental panel for climate change. Geneva: IPCC Secretariat; 2008.
5. Todd MC, Taylor RG, Osborn TJ, Kingston DG, Arnell NW, Gosling SN. Uncertainty in climate change impacts on basin-scale freshwater resources – preface to the special issue: the QUEST-GSI methodology and synthesis of results. *Hydrology and Earth System Sciences*. 2011;15:1035–1046. DOI: 10.5194/hess-15-1035-2011.
6. Notter B, Hans H, Wiesmann U, Ngana JO. Evaluating watershed service availability under future management and climate change scenarios in the Pangani Basin. *Physics and Chemistry of the Earth*. 2013;61-62:1-11. DOI: 10.1016/j.pce.2012.08.017
7. Randall DA, Wood RA, Bony S, Colman R, Fife J, et al. Climate models and their evaluation, in *Climate Change: The Physical Science Basis*. Contribution of Working Group 1 to the AR4: Cambridge Univ. Press; 2007.
8. Perkins SE, Pitman AJ, Holbrook NJ, Mcaneney J. Evaluation of the AR4 climate models' simulated daily maximum temperature, minimum temperature, and precipitation over Australia using probability density functions. *Journal of Climate*. 2007;20:4356-4376. DOI: 10.1175/JCLI4253.1.
9. Frich P, Alexander LV, Della-Marta P, Gleason B, Haylock M, Klein AMGT, et al. Observed coherent changes in climatic extremes during the second half of the twentieth century. *Climate Research*. 2002;19:193–212.
10. Wilby RL, Wigley TML. Downscaling general circulation mode output: a review of methods and limitations. *Progress in Physical Geography*. 1997;21:530–548. DOI: 10.1177/030913339702100403.
11. Prudhomme C, Reynard N, Crooks S. Downscaling of global climate models for flood frequency analysis: where are we now? *Hydrological Processes*. 2002;16:1137–1150. DOI: 10.1002/hyp.1054.

12. Fowler HJ, Blenkinsop S, Tebaldib C. Review: Linking climate change modelling to impacts studies: recent advances in downscaling techniques for hydrological modelling. *International Journal of Climatology*. 2007;27:1547–1578. DOI: 10.1002/joc.1556.
13. Arnold JG, Srinivasan R, Muttiah RS, Williams JR. Large area hydrologic modelling and assessment. Part 1: Model development. *Journal of the American Water Resources Association*. 1998;34(1):73–89.
14. Neitsch SL, Arnold JG, Kiniry JR, Williams JR, King KW. Soil and water assessment tools: Theoretical documentation version. Report No: 061. 808 East Blackland Road-temple (TX): Grassland, Soil and Water Research Laboratory, ARS; 2005.
15. SCS (USDA Soil Conservation Service). *National Engineering Handbook*. Section 4: Hydrology. 1972;4-10.
16. Ndomba PM, Birhanu BZ. Problems and prospects of SWAT model applications in NILOTIC catchments: A review. *Nile Basin Water Engineering Scientific Magazine*. 2008;1.
17. Yang J, Reichert P, Abbaspour KC, Jun X, Hong Y. Comparing uncertainty analysis techniques for a SWAT application to the Chaohe Basin in China. *Journal of Hydrology*. 2008;358:1-23. DOI: 10.1016/j.jhydrol.2008.05.012.
18. Abbaspour KC, Van Genuchten MT, Schulin R, Schlaeppli E. A sequential uncertainty domain inverse procedure for estimating subsurface flow and transport parameters. *Water Resources Research*. 1997;33(8):1879–1892.
19. Nash JE, Sutcliffe JV. River flow forecasting through. Part I. A conceptual models discussion of principles. *Journal of Hydrology*. 1970;10:282–290.
20. Legates DR, McCabe GJ. Evaluating the use of “goodness-of-fit” measures in hydrologic and hydroclimatic model validation. *Water Resources Research*. 1999;35(1):233-241. DOI: 10.1029/1998WR900018.
21. United Republic of Tanzania. *The Tanzania Development Vision 2025*. Dar es Salaam, Tanzania; 1999.
22. Zhu HY, Jia SF. Uncertainty in the spatial interpolation of rainfall data. *Progress in Geography*. 2004;23(2):34–42. DOI: 10.11820/dlxxjz.2004.02.005.
23. Lin XS, Yu Q. Study on the spatial interpolation of agroclimatic resources in Chongqing. *Journal of Anhui Agricultural Science*. 2008;36(30):13431–13463. Chinese.
24. Nicks AD. Stochastic generation of the occurrence, pattern, and location of maximum amount of daily rainfall. In *Proc. Symp. Statistical Hydrology*, Aug.-Sept. 1971. Tuscon, AZ. U.S. Department of Agriculture. 1974;1275:154-171.
25. Anyamba A, Tucker CJ, Mahoney R. From El Nino to La Nina: Vegetation Response Patterns over East and Southern Africa during the 1997-2000 period. *Journal of Climate*. 2002;15:3096-3103. Available: [http://dx.doi.org/10.1175/1520-0442\(2002\)015<3096:FENOTL>2.0.CO;2](http://dx.doi.org/10.1175/1520-0442(2002)015<3096:FENOTL>2.0.CO;2)
26. IPCC. *The scientific Basis. Contribution of working group I to the third assessment report of the intergovernmental panel on climate change*. New York. Cambridge University Press; 2007.
27. Graham LP, Andréasson J, Carlsson B. Assessing climate change impacts on hydrology from an ensemble of regional climate models, model scales and linking methods-A case study on the Lule River basin. *Climatic Change*. 2007;81(S1):293–307. DOI: 10.1007/s10584-006-9215-2.
28. Sperna WFC, Van Beek LPH, Kwadijk JCJ, Bierkens MFP. The ability of a GCM-forced hydrological model to reproduce global discharge variability. *Hydrology and Earth System Science*. 2010;14(8):1595–1621. DOI: 10.5194/hess-14-1595-2010.

29. Eisner S, Voss F, Kynast E. Statistical bias correction of global climate projections – consequences for large scale modeling of flood flows. *Advances in Geosciences*. 2012;31:75–82. DOI: 10.5194/adgeo-31-75-2012.
30. Watanabe S, Kanae S, Seto S, Yeh PJF, Hirabayashi Y, Oki T. Intercomparison of bias-correction methods for monthly temperature and precipitation simulated by multiple climate models. *Journal of Geophysical Research*. 2012;117:D23114. DOI: 10.1029/2012JD018192.
31. Leander R, Buishand TA. Resampling of regional climate model output for the simulation of extreme river flows. *Journal of Hydrology*. 2007;332(3–4):487–496. DOI: 10.1016/j.jhydrol.2006.08.006.
32. Leander R, Buishand T, Vandenhurk B, Dewit M. Estimated changes in flood quantiles of the river Meuse from resampling of regional climate model output. *Journal of Hydrology*. 2008;351(3–4):331–343. DOI: 10.1016/j.jhydrol.2007.12.020.
33. Van Pelt SC, Kabat P, ter Maat HW, van den Hurk BJM, Weerts AH. Discharge simulations performed with a hydrological model using bias corrected regional climate model input. *Hydrology and Earth System Science*. 2009;13(12):2387–2397. DOI: 10.5194/hess-13-2387-2009.
34. Hurkmans R, Terink W, Remko U, Torfs P. Changes in streamflow dynamics in the Rhine Basin under three high-resolution regional climate scenarios. *Journal of Climate*. 2010;23(3):679–699. Available: <http://dx.doi.org/10.1175/2009JCLI3066.1>
35. Terink W, Hurkmans RTWL, Torfs PJF, Uijlenhoet R. Evaluation of a bias-correction method applied to downscaled precipitation and temperature reanalysis data for the Rhine basin. *Hydrology and Earth System Sciences*. 2010;7(1):221–267. DOI: 10.5194/hessd-7-221-2010.
36. Santhi C, Arnold JG, Williams JR, Dugas WA, Srinivasan R, Hauck LM. Validation of the SWAT model on a large river basin with point and nonpoint sources. *Journal of the American Water Resources Association*. 2001;37(5):1169–1188. DOI: 10.1111/j.1752-1688.2001.tb03630.x.
37. Benaman J, Christine AS, Douglas AH. Calibration and validation of soil and water assessment tool on an agricultural watershed in upstate New York. *Journal of Hydrologic Engineering, ASCE*. 2005;10(5):363-374. Available: [http://dx.doi.org/10.1061/\(ASCE\)1084-0699\(2005\)10:5\(363\)](http://dx.doi.org/10.1061/(ASCE)1084-0699(2005)10:5(363))
38. Moriasi DN, Arnold JG, Van Liew MW, Binger RL, Harmel RD, Veith T. Model evaluation guidelines for systematic quantification of accuracy in watershed simulations. *Transactions of the ASABE*. 2007;50(3):885-900.
39. Saleh A, Arnold J, Gassman PWA, Hauck L, Rosenthal W, Williams J, et al. Application of SWAT for the upper North Bosque River Watershed. *Transactions of the ASAE*. 2000;43:1077–1087.
40. Rossi CG, Dybala TJ, Moriasi DN, Arnold JG, Amonett C, Marek T. Hydrologic calibration and validation of the soil and water assessment tool for the Leon River watershed. *Journal of Soil and Water Conservation*. 2008;6:533–541. DOI: 10.2489/jswc.63.6.533.

© 2014 Wambura; This is an Open Access article distributed under the terms of the Creative Commons Attribution License (<http://creativecommons.org/licenses/by/3.0>), which permits unrestricted use, distribution, and reproduction in any medium, provided the original work is properly cited.

*Peer-review history:*

*The peer review history for this paper can be accessed here:*  
<http://www.sciencedomain.org/review-history.php?iid=857&id=10&aid=7008>